Overtone-induced isomerization of allyl isocyanide

Jeffrey Segall[a] and Richard N. Zare
Department of Chemistry, Stanford University, Stanford, California 94305

(Received 20 May 1988; accepted 21 July 1988)

The rate of isomerization of allyl isocyanide to allyl cyanide is monitored using Stern–Volmer kinetics when various features of the 5–0 and 6–0 C–H overtone stretch region are excited. Previously, Reddy and Berry found that the isomerization rates varied from band to band and that the variations were not monotonic with excitation energy. They attributed this behavior to nonstatistical effects. It is found in this study that the isomerization rates vary within an overtone band by up to a factor of 1.8, in addition to the variations from band to band seen previously. This observation rules out the possibility that the overtone bands are purely lifetime broadened. In addition, the photoisomerization rate increases with increasing temperature. An increase of 60 K increases the photolysis yield in the 5–0 C–H region by a factor of 3–4, while increases in the 6–0 C–H region are smaller, 25%–60%. These effects can be qualitatively explained if the overtone spectrum of allyl isocyanide is inhomogeneously broadened because of the presence of vibrational "hot bands." In this case, molecules excited by the photolysis laser will have varying amounts of initial thermal energy depending on where the laser is tuned within a band. A simple model for the effects of hot bands on the isomerization rate is in good agreement with experimental results. It is not necessary to invoke nonstatistical effects in order to explain the observed overtone-pumped isomerization rates of allyl isocyanide.

I. INTRODUCTION

In the 20 years since the local mode model for high vibrational overtones was proposed to explain the weak visible absorption bands in benzene,[1] there has been a remarkable number of experimental and theoretical studies of vibrational overtones in polyatomic molecules.[2] Benzene and many other polyatomic molecules containing an X–H bond (X = C, N, O, Si, etc.) show a series of progressively weaker absorption bands following the relation

$$\nu_{n-0} = n\omega_e - n^2\omega_e x_e, \quad n = 1,2,3,\ldots .$$

This behavior is similar to the vibrational progressions seen in diatomics, such as HCl.[3] Observation of these vibrational overtones of the fundamental (1–0) X–H transition led to the conclusion that this quasidiatomic behavior was indicative of a localized, highly excited motion of the molecule. Subsequent theoretical work supported the concept of highly excited states largely uncoupled from the rest of the molecule.[4,5] Localization of vibrational energy in a bond is contrary to a key tenet of statistical unimolecular reaction rate (RRKM) theory,[6] which states that energy flows rapidly compared with the time necessary for unimolecular reaction. Support for this assumption came from experiments designed to prepare site selectively energized molecules using techniques such as chemical activation and IR multiphoton excitation. These experiments yielded results that could be successfully accounted for with RRKM theory. Nevertheless, interpretation of the results of such experiments often involved extensive ensemble averaging, which made comparison with theory more complicated and less meaningful. Overtone pumping held the promise of cleanly exciting molecules with a narrow distribution of vibrational energy isolated in a particular molecular motion. A molecule with vibrational energy localized within a bond for a sufficient period of time would be new and might be expected to behave differently from a molecule with a statistical distribution of energy. Furthermore, as first expressed by Reddy and Berry,[7,8] it was hoped that by choosing a particular vibrational motion, the localized excitation could be exploited to enhance chemical reactivity or to promote one reaction channel relative to another.

However, with few exceptions, experiments designed to look for "mode specific chemistry" prepared by overtone excitation have concluded that these reactions proceed statistically and not mode specifically. For example, the work of Jasinski, Frisoli, and Moore[9–12] on a series of cycloalkenes revealed that the unimolecular reaction rate measured upon exciting a C–H oscillator near the reaction site showed no enhancement relative to excitation in another part of the molecule. The measured reaction rates in these systems increased monotonically with excitation energy and seemed to be completely insensitive to the nature of the mode excited. These results were interpreted as evidence for very rapid (< 1 ps) decay of the initially prepared overtone state into various "bath modes" by intramolecular vibrational redistribution (IVR), which was consistent with the observation of extremely broad overtone linewidths seen in most polyatomic molecules.[13]

Not all experiments led to this conclusion, however. Chandler, Farneth, and Zare[14] reported observation of a fast, nonstatistical component to the 5–0 O–H overtone pumped decomposition of tert-butyl hydroperoxide. Later, Chuang *et al.*[15] studied the decomposition of this molecule induced by pumping the 6–0 O–H stretch. They found an even more dramatic effect. However, Klenerman, Gutow,

[a] Present address: Department of Chemistry, University of Southern California, Los Angeles, CA 90089.

 0021-9606/88/215704-11$02.10

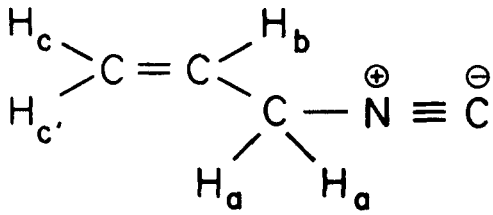

FIG. 1. Molecular structure of allyl isocyanide: H_a = methylenic hydrogen; H_b = nonterminal olefinic hydrogen; and H_c,$H_{c'}$ = terminal olefinic hydrogen.

and Zare[16] found that the rapid component at the 6–0 O–H level was due to contributions from excited electronic states, whereas pumping at the 5–0 O–H level was free of this complication. Although the pumped O-H bond is adjacent to the reaction coordinate, the O–O bond, and one might expect a large enhancement of the decomposition rate from molecules with a nonergodic distribution of vibrational energy, the nonstatistical contribution to the 5–0 O–H pumped decomposition rate was estimated to be only 1%.

Another system for which nonstatistical effects in an overtone-pumped molecule have been reported[17] is the photoisomerization of allyl isocyanide and this system is the focus of the present study. Allyl isocyanide (see Fig. 1 for molecular structure) is a member of a class of compounds known as isonitriles, which are the only known stable molecules to possess a formally divalent carbon.[18] The isomerization reaction of isonitriles into the corresponding nitriles

$$R\text{–}N{\equiv}C \rightarrow R\text{–}C{\equiv}N$$

has been known for almost a century. The isomerization of the simplest isonitrile, hydrogen isocyanide (R=H), has been the subject of considerable theoretical,[19,20] but not experimental, work, as HNC has never been isolated in the gas phase. The rearrangement of methyl isocyanide ($R{=}CH_3$) may well be the most thoroughly studied unimolecular isomerization reaction, both theoretically and experimentally.[7,8,21–27]

However, allyl isocyanide remained obscure until Reddy and Berry studied its overtone-induced photoisomerization.[17] In this work, the authors assigned the three broad absorption features in the 5–0, 6–0, and 7–0 C–H stretch region to the three different C–H oscillators in allyl isocyanide (see Fig. 1). Next, they tuned their laser to each of these nine absorption maxima and monitored the yield of allyl cyanide at these wavelengths as a function of pressure. From a Stern–Volmer analysis of inverse yield vs pressure (see Sec. III B), they calculated a unimolecular isomerization rate for excitation at each of the nine absorption peaks. Reddy and Berry observed a nonmonotonic variation in the photoisomerization rate with the photolysis photon energy. They concluded that this effect was attributable to a nonergodic distribution of vibrational energy in the overtone-pumped allyl isocyanide molecule. The observed isomerization rates were seen to vary by approximately a factor of two or three within a given overtone region. Observation of an enhancement in the reaction rate by pumping different C–H oscillators in allyl isocyanide is somewhat surprising because the C–H stretching motions involved are far removed from the reaction coordinate, which is believed to be a rotation of the cyano group (see Sec. III E). Because of the importance of possible mode specific effects and the controversy surrounding the results and conclusions of the Reddy and Berry work,[28] we undertook to restudy the overtone-induced isomerization of allyl isocyanide.

II. EXPERIMENTAL

A. Sample preparation

Allyl isocyanide, $CH_2{=}CHCH_2N{\equiv}C$ (Fig. 1), was prepared according to the method of Hartman and Weinstock[29] by condensation of allyl amine, $CH_2{=}CHCH_2NH_2$, and methyl formate, $HCOOCH_3$, to yield allyl formamide, $CH_2{=}CHCH_2NHCOH$. The amide was then dehydrated with *p*-toluenesulfonyl chloride and tributylamine under reduced pressure to form allyl isocyanide (bp 395 K). The identity and purity of the obtained compound were determined by NMR and gas chromatography. Typical purity was > 98%, with CH_3OH and CH_3COCH_3 being the major contaminants. Sample handling was done on a glass vacuum line equipped with a digital pressure gauge (Wallace and Tiernan 66-200). All samples were thoroughly degassed by several freeze–pump–thaw cycles. Special care must be used in handling isonitriles because of their "vile odor."[30]

B. Photoacoustic spectroscopy

Laser photoacoustic spectroscopy techniques have been described in detail elsewhere.[31–33] Photoacoustic spectra were obtained by placing a cell equipped with quartz windows at Brewster's angle and affixed with a microphone (Knowles 1759) inside the cavity of a linear dye laser (Spectra-Physics 375). The intracavity power of the laser was enhanced by using a high reflector in place of an output coupler. Tuning of the laser was achieved by rotating a three-plate birefringent filter (resolution 2 cm^{-1}). The dye laser was modulated by mechanically chopping the pump laser (Spectra-Physics 165 or 171). The microphone signal at the chopping frequency was detected using a lock-in amplifier (PAR 192 and 124A). The intracavity power was measured from a reflection off the photoacoustic cell.[14] The measured power was smoothed to compensate for the spurious power modulation in reflected beams from inside the laser cavity.[34] Part of the output beam was directed into a neon hollow cathode lamp (Perkin-Elmer 303-6017) to provide absolute wavelength calibration. The remaining output beam was passed through an etalon for relative frequency spacing. Tuning accuracy was typically within the bandwidth of the laser, approximately 1 cm^{-1}. All signals were fed into a computer (IBM PC-XT) for storage and analysis. Absorption cross sections were measured using mixtures of allyl isocyanide and methane.[35] While uncertainty in the absolute cross section may be as high as 30%, relative uncertainty in the spectra is less than 5%.

C. Photoisomerization

Overtone-pumped photoisomerization experiments have also been described previously.[7–17,25,36] Briefly, a known

pressure of allyl isocyanide was introduced into a glass photolysis cell, which was fitted with Brewster's angle windows. For experiments above room temperature, the cell was wrapped with heating tape. The temperature was monitored using a thermocouple. The cell was then placed inside the dye laser cavity. The dye laser wavelength was controlled as described above. The sample was photolyzed for a period of time which ranged from 5 min to 4 h. This was sufficient to give approximately 1% yield of allyl cyanide, depending on sample pressure and photolysis wavelength. Sample analysis was done with a gas chromatograph (Hewlett–Packard 5890A) interfaced by a six-port valve to a 2 ml sample loop and a vacuum line. Good separation of allyl isocyanide and allyl cyanide was achieved with a 3 ft × 1/4 in. stainless steel column of 10% Carbowax 20M on Chromosorb WHP (Alltech Associates) maintained at 100 °C with a 40 ml/min He flow rate. Typical retention times for the isocyanide and cyanide were 3.3 and 5.3 min, respectively. A flame ionization detector (FID) was used to detect the effluents from the column. Because both product and reactant adsorb onto glass and metal surfaces, the chromatographic peaks were very asymmetric. Therefore, integration of the FID signal (Hewlett–Packard 3392A) was useful for quantitative analysis of the photolyzed sample. Calibration of the FID signal intensity was determined and periodically checked by injecting gas mixtures of approximately 1% allyl cyanide in allyl isocyanide. Photolyses at a given wavelength and pressure were performed and analyzed four to six times to provide mean values and standard deviations. Typical error bars are ~5%. Test runs where allyl isocyanide was maintained at either room temperature or at temperatures up to 80 °C in the photolysis cell without laser irradiation revealed no "dark" or background reaction.

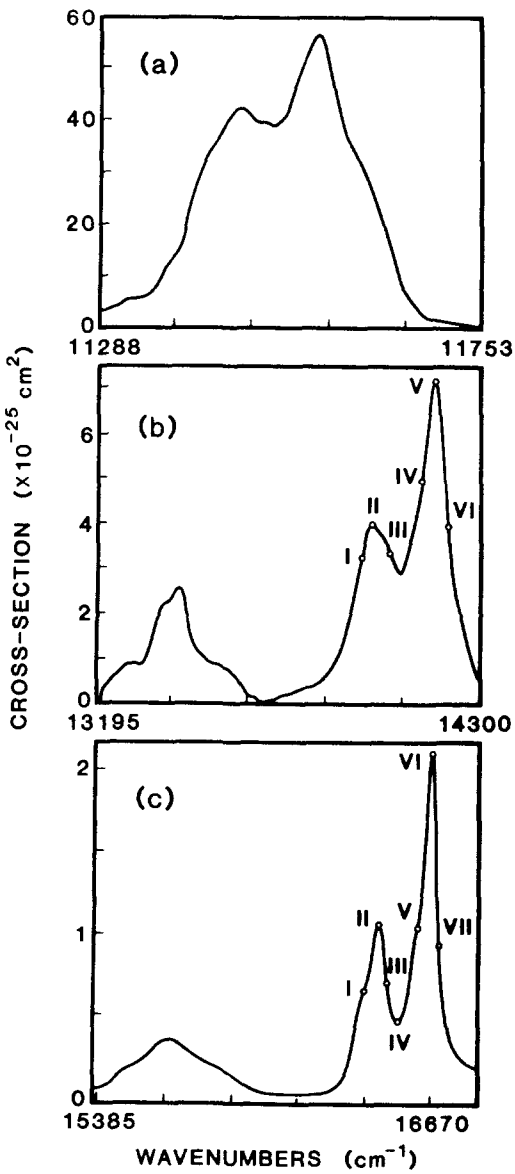

FIG. 2. Photoacoustic spectra of allyl isocyanide: (a) the 4–0 C–H stretch region; (b) the 5–0 C–H stretch region; and (c) the 6–0 C–H stretch region from Ref. 17. In (b) and (c) Roman numerals indicate photolysis energies; see Sec. III C. Typical sample pressures are 10 Torr allyl isocyanide and 200 Torr N_2.

III. RESULTS

A. Allyl isocyanide C–H overtone spectra

Photoacoustic absorption spectra of the 4–0, 5–0, and 6–0 C–H stretch regions of allyl isocyanide are shown in Fig. 2.[37] In the 5–0 and 6–0 C–H stretch spectra, three broad absorption features appear, as reported by Reddy and Berry.[17] They assigned these three features to C–H stretch contributions from the aliphatic hydrogens, the lone nonterminal olefinic hydrogen, and the terminal olefinic hydrogens (see Fig. 1), in order of increasing energy. This assignment was based on the assigned fundamental spectrum of allyl cyanide,[38] overtone spectra of deuterated analogs of propene,[17] and trends seen in alkanes and alkenes.[39] The C–H absorption data for allyl isocyanide, including the 7–0 data from Reddy and Berry,[17] are represented in a Birge–Sponer plot in Fig. 3. The absorption maxima fall along three lines, characteristic of three localized anharmonic oscillators.[4,5] Best fits to the natural frequency ω_e and the anharmonicity $\omega_e x_e$ are given in Table I. In the 4–0 C–H overtone spectrum

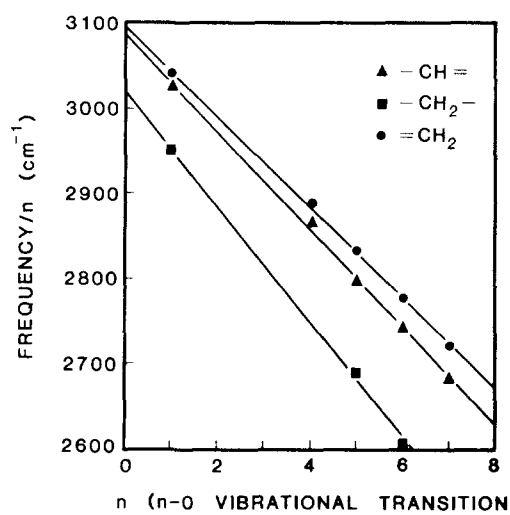

FIG. 3. Birge–Sponer plot for C–H fundamentals (see Ref. 37) and overtones of allyl isocyanide. Data for 7–0 absorptions are from Ref. 17.

TABLE I. Anharmonic oscillator constants for C–H stretch absorptions in allyl isocyanide.

Peak[a]	ω_e (cm^{-1})	$\omega_e x_e$ (cm^{-1})
a	3019	− 67.5
b	3085	− 56.7
c	3095	− 53.0

[a] See Fig. 1 for designation for the C–H oscillators.

[Fig. 2(c)], which has not previously been published, only the two higher energy features appear because of the limited tuning range of the laser dye.

B. Photoisomerization kinetics

Combining the Stern–Volmer mechanism

$$A + h\nu \xrightarrow{k_1} A^* \quad \text{photoactivation,} \tag{1}$$

$$A^* + M \xrightarrow{k_2} A + M \quad \text{collisional deactivation,} \tag{2}$$

$$A^* \xrightarrow{k_3(h\nu)} P \quad \text{unimolecular reaction} \tag{3}$$

with the steady state assumption for A*, gives

$$\frac{-d[A]}{dt} = \frac{k_1 k_3(h\nu)}{k_2[M] + k_3(h\nu)}[A][h\nu]. \tag{4}$$

The unimolecular reaction rate constant is written as $k_3(h\nu)$ since we measure this quantity as a function of the excitation energy $h\nu$. Integrating this rate equation from $t = 0$ to τ, where τ is the photolysis time, and neglecting terms of order $[P]^2/[A]_0^2$ and higher after expanding the logarithm yields

$$k_{app} = \frac{[P]}{[A]_0[h\nu]\tau}, \tag{5}$$

where

$$k_{app} = \frac{k_1 k_3(h\nu)}{k_2[M] + k_3(h\nu)}. \tag{6}$$

Neglecting higher orders of $[P]/[A]_0$ is an excellent approximation in this case as the product yield was always roughly 1%.

All of the quantities on the right-hand side of Eq. (5) are directly measurable except $[h\nu]$. The latter can be calculated from the relation

$$[h\nu] = \frac{P_{out}}{hc\nu TA}, \tag{7}$$

where P_{out} is the measured output from the laser end mirror, c is the speed of light, ν is the photolysis frequency, T is the fractional transmission of the end mirror, and A is the cross sectional area of the photolysis cell.

From Eq. (6), we can write

$$k_{app}^{-1} = \frac{k_2}{k_1 k_3(h\nu)}[M] + \frac{1}{k_1} \tag{8}$$

or

$$k_1/k_{app} = \frac{k_2}{k_3(h\nu)}[M] + 1. \tag{9}$$

Equation (8) shows that k_{app}^{-1} should vary linearly with pressure and have a zero-pressure intercept value inversely proportional to the photoactivation rate constant k_1. This quantity can be determined independently by the relation

$$k_1 = \sigma(\nu)c, \tag{10}$$

where $\sigma(\nu)$ is the absorption cross section at the photolysis frequency ν. A reduced Stern–Volmer plot of k_1/k_{app} vs pressure will have slope $k_2/k_3(h\nu)$. Thus, the unimolecular reaction rate constant $k_3(h\nu)$ can be determined if the collisional deactivation rate constant k_2 is known.

C. Room temperature photoisomerization results

Figure 4 shows both types of Stern–Volmer plots for the photoisomerization of allyl isocyanide at seven wavelengths in the 6–0 C–H stretch region. The data show no significant deviations from linearity over the pressure range studied.

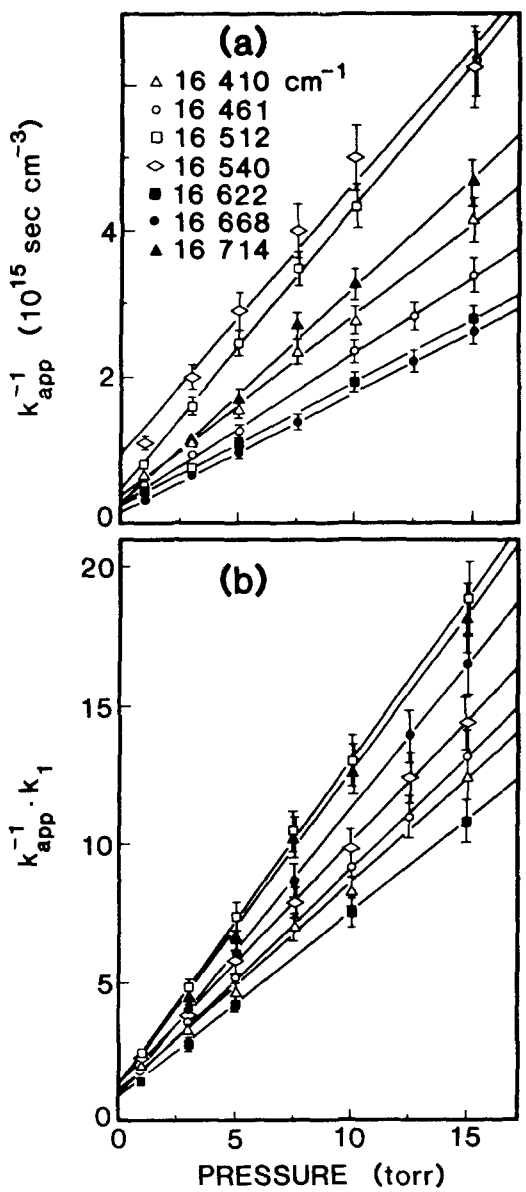

FIG. 4. Photolysis data in the 6–0 C–H stretch region: (a) Stern–Volmer plot; (b) reduced Stern–Volmer plot. Data are shown with 7% error bars.

TABLE II. Isomerization rates and absorption cross sections from 6–0 C–H region photolyses.

			$k_3(h\nu)$ ($\times 10^6\ s^{-1}$)[c]	
ν(cm^{-1})	σ(mbar)[a]	σ(mbar)[b]	This work	Ref. 17
16 410	100	93	7.3	
16 461	130	130	6.8	10.0
16 512	100	75	4.6	
16 540	66	49	6.8	
16 622	130	150	8.5	
16 668	210	240	6.0	7.7
16 714	130	120	4.8	

[a] Spectroscopic cross section (see the text) mbar $= 10^{-27}$ cm^2.
[b] Cross section inferred from Stern–Volmer intercept.
[c] Assumes $k_2 = 1.65\times10^{-10}$ cm^3 s^{-1}.

TABLE III. Isomerization rates and absorption cross sections from 5–0 C–H region photolyses.

			$k_3(h\nu)$ ($\times 10^5\ s^{-1}$)[c]	
ν(cm^{-1})	σ(mbar)[a]	σ(mbar)[b]	This work	Ref. 17
13 952	310	24	(7.1)[d]	
13 986	420	60	(7.7)[d]	5.0
14 040	360	30	(10.8)[d]	
14 128	470	280	12.0	
14 168	710	580	10.3	7.3
14 206	410	350	7.5	

[a] Spectroscopic absorption cross section (see the text). mbar $= 10^{-27}$ cm^2.
[b] Cross section inferred from Stern–Volmer intercepts (see the text).
[c] Assumes $k_2 = 1.65\times10^{-10}$ cm^3 s^{-1}.
[d] The photolysis data at 14 040 cm^{-1} and below are more difficult to interpret. See Sec. III C.

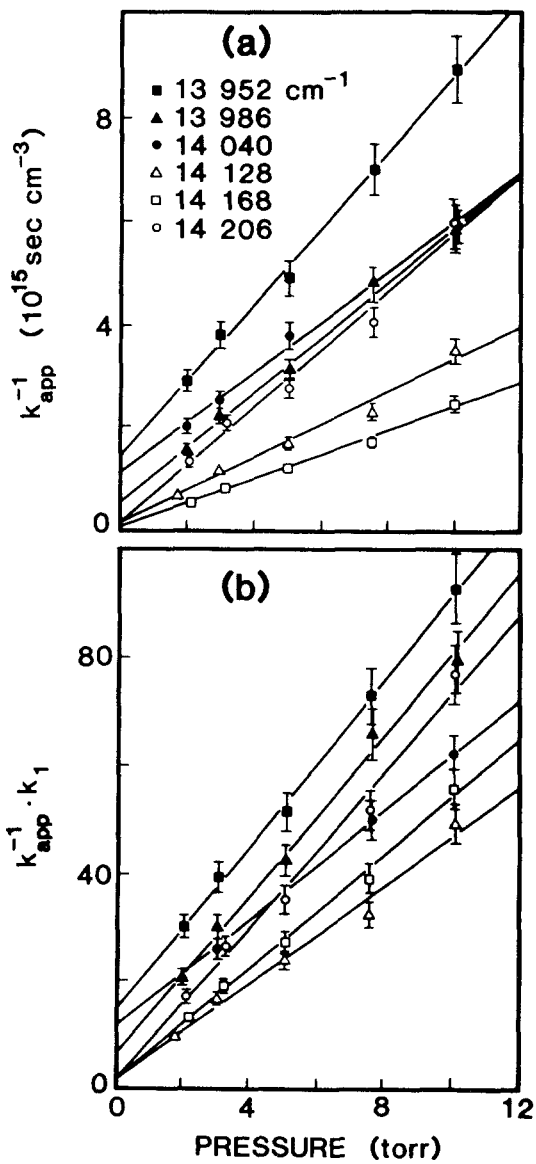

FIG. 5. Photolysis data in the 5–0 C–H stretch region: (a) Stern–Volmer plot; (b) reduced Stern–Volmer plot. Data are shown with 7% error bars.

Figure 4(a) shows that the extrapolated intercept value varies with photolysis wavelength, approximately mirroring changes in the absorption intensity. In the reduced Stern–Volmer plot [Fig. 4(b)], these differences are factored out and the slope depends only on the ratio of rate constants $k_2/k_3(h\nu)$. As Fig. 4(b) indicates, the ratio $k_2/k_3(h\nu)$ is seen to vary dramatically and nonmonotonically with excitation energy. If the collisional deactivation rate is assumed to be constant over this 300 cm^{-1} energy range (see Sec. IV A), $k_3(h\nu)$ must vary nonmonotonically with excitation energy. Remarkably, photolysis to the red of an overtone peak shows a faster isomerization rate and photolysis to the blue results in a slower rate than photolysis at the absorption maximum. A summary of 6–0 C–H photolysis data is given in Table II. For comparison, the $k_3(h\nu)$ data of Reddy and Berry[17] at 16 461 and 16 668 cm^{-1} are also presented. The agreement is good in view of the estimated uncertainties, which are 10%–20% for the Reddy and Berry data and 5%–10% in the present work. The $k_3(h\nu)$ values shown are calculated with $k_2 = 1.65\times10^{-10}$ cm^3 s^{-1}, which is calculated from a hard-sphere collision diameter of 3.5 Å. The photoisomerization rate constants from Reddy and Berry are rescaled to this value of k_2 for comparison with the present results. See Sec. IV for a discussion of the collisional deactivation rate.

Stern–Volmer plots for six wavelengths in 5–0 C–H stretch are shown in Fig. 5. Differences from the 6–0 data are immediately apparent. In Fig. 5(b), we see that photolyses at 14 040 cm^{-1} and lower energy yield Stern–Volmer plots that extrapolate to zero-pressure intercept values higher than those calculated from the absorption cross section. Thus, the absorption cross section inferred from the kinetic measurements is considerably smaller than the cross section measured photoacoustically, as shown in Table III. However, excitation at 14 128, 14 168, and 14 206 cm^{-1} yields extrapolated cross sections in good agreement with the spectroscopically measured values. The $k_3(h\nu)$ values from Reddy and Berry at 13 986 and 14 168 cm^{-1} are also represented in Table III. There is agreement at 14 168 cm^{-1} to within the estimated errors of the data sets, but the disagreement is considerably greater at 13 986 cm^{-1}. We note, how-

ever, that our room temperature results below 14 128 cm^{-1} were somewhat less reproducible than at higher photolysis energies. The very strong temperature dependence at 14 040 cm^{-1} shown in Fig. 8(a) indicates a possible source of the greater uncertainties in this wavelength range.

D. Elevated temperature photoisomerization results

The effects of heating the photolysis cell during irradiation are seen in Fig. 6. With the photolysis laser tuned to 14 040 cm^{-1} [Fig. 6(a)], the slope in this k_{app}^{-1} vs pressure plot is seen to change markedly with temperature. Furthermore, the extrapolated k_{app}^{-1} intercept also decreases upon heating to 353 K. This decrease brings the intercept value closer to that predicted from the photoacoustic spectrum. In Figs. 6(b) and 6(c), the photolysis laser is tuned to two wavelengths in the 6–0 C–H stretch region, 16 672 and 16 622 cm^{-1}. Here, effects upon heating are more subtle. In both cases, the intercepts do not change appreciably. At 16 672 cm^{-1}, there seems to be a decrease in slope as the temperature is increased from 298 to 333 K, but the effect is close to the experimental error in magnitude. However, a definite decrease in slope of the Stern–Volmer plot at 16 622 cm^{-1} is seen upon heating from 298 to 353 K [Fig. 6(c)].

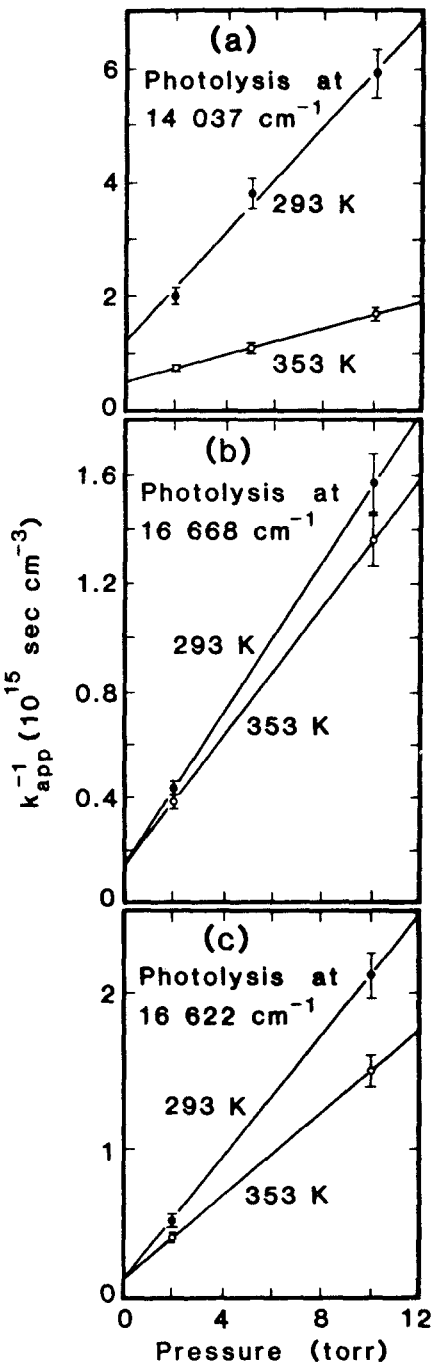

FIG. 6. Temperature dependence in allyl isocyanide photoisomerization: photolyses at (a) 14 037; (b) 16 668; and (c) 16 622 cm^{-1}.

E. Calculated unimolecular reaction rate: RRKM theory

Before proceeding with a calculation of the statistical reaction rate as a function of internal energy, the nature of the transition state between reactant and product must be understood. Because of its unique structure, allyl isocyanide appears to have two possible reaction pathways to allyl cyanide. In the case of alkyl and aryl isonitrile rearrangements there is considerable theoretical[26,27] and experimental[40] evidence that the reaction is an example of the Wagner–Meerwein 1–2 shift,[21] i.e., rotation of the R substituent around the C≡N group, with very little charge separation developing between the R and cyano groups [see Fig. 7(a)]. Alternatively, because of its unsaturated bond, allyl isocyanide could also form product via a five-membered intermediate as shown in Fig. 7(b). The only available experimental evidence on the reaction mechanism is the thermal activation work by Glionna and Pritchard,[41] who report an activation energy $E_a^{\infty} = 170.7 \pm 2.5$ kJ/mol and a $\log(A_{\infty})$ factor of 14.77 ± 0.30. For methyl isocyanide isomerization,[21,22] which is known to react by the mechanism shown in Fig. 7(a), the Arrhenius parameters are $E_a^{\infty} = 160$ kJ/mol and

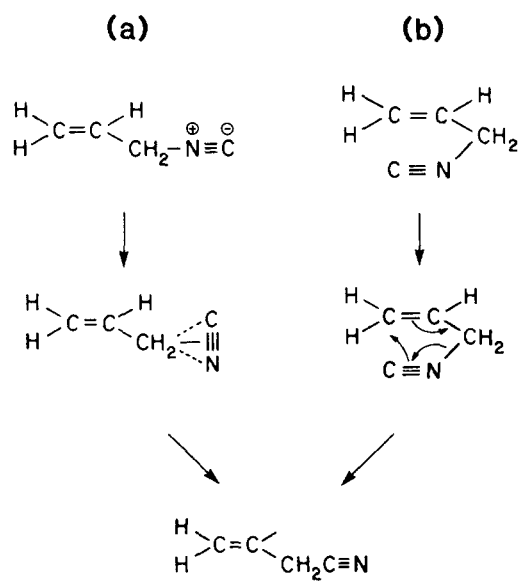

FIG. 7. Possible reaction pathways for allyl isocyanide isomerization to allyl cyanide: (a) 1–2 Wagner–Meerwin shift, i.e., cyano group rotation; (b) five-membered ring transition state.

$\log(A_\infty) = 13.6$. Glionna and Pritchard argue that the greater E_a^∞ and $\log(A_\infty)$ values for the allyl isocyanide isomerization indicate that the electrocyclic mechanism shown in Fig. 7(b) is unimportant. However, the reported $\log(A_\infty)$ of 14.77 seems to be anomalously large for an isomerization reaction because $\log(A_\infty)$ values greater than ~ 13.5 imply a gain in entropy from the reactant to the transition state. Examination of the thermal rate data reported by Glionna and Pritchard reveals that the data are also well fit by the Arrhenius parameter values $E_a^\infty = 161$ kJ/mol and $\log(A_\infty) = 13.5$. We prefer these values as they appear to be more physically reasonable. The thermal rate data does not provide definitive evidence for the nature of the reaction mechanism. However, because of the great similarity between our preferred values for the Arrhenius parameters for allyl isocyanide and those for methyl isocyanide, we choose to model the activated complex as analogous to that for methyl isocyanide and other isonitrile rearrangements, as shown in Fig. 7(a).

Calculation of the statistical isomerization rate uses the well-known RRKM expression[6]

$$k(E) = L^\ddagger \frac{Q^+}{Q} \frac{\Sigma P(E - E_0)}{hN(E)}, \tag{11}$$

where $L^\ddagger$ is the reaction path degeneracy, Q^+ and Q are the rotational partition functions for the transition state complex and the molecule, respectively, E is the vibrational energy, E_0 is the critical energy for reaction, $\Sigma P(E - E_0)$ is the sum of states of the activated complex, h is Planck's constant, and $N(E)$ is the density of states of the molecule. The computation used the Beyer–Swinehart algorithm for direct counting of states.[42] Normal mode frequencies for allyl isocyanide are taken from studies of allyl cyanide,[38] with a small correction in the C≡N stretch frequency from 2247 to 2150 cm^{-1}. The close similarity in the infrared spectra of $CH_3N{\equiv}C$[43] and $CH_3C{\equiv}N$,[44] with the exception of the C≡N stretch frequency, suggests that this is a good approximation. Frequencies for the reactive complex are identical except that the reaction coordinate is removed and the C≡N and C–N stretch frequencies are lowered from 2150 to 2000 cm^{-1} and from 937 to 600 cm^{-1}, respectively, reflecting a weakening of these bonds at the saddle point. This treatment is consistent with both the calculated Hartree–Fock transition state frequencies for methyl isocyanide isomerization[27] and the successful RRKM calculations on methyl isocyanide thermal isomerization.[22] The experimental high pressure activation energy $E_a^\infty = 161$ kJ/mol is corrected for temperature[45] to give a critical energy for reaction of $E_0 = 160$ kJ/mol. It is worth noting that this experimentally based value for the reaction barrier, which was unavailable to Reddy and Berry,[17] differs substantially from their estimate for the critical energy $E_0 = 151$ kJ/mol. Therefore, our calculated rates are three to seven times slower in the energy range 15 000 to 18 000 cm^{-1} than those calculated previously. Adiabatic rotational energy contributions are expected to be very small[46] and are ignored. Similarly, the effects of anharmonicity have been shown to be small in methyl isocyanide isomerization[23] and are likely to be considerably less in the case of allyl isocyanide, as it has double the number of normal modes. This reduces the average amount of energy in each mode, thus decreasing the contribution of anharmonicity. The reaction path degeneracy is three, by analogy to the RRKM modeling of ethyl isocyanide.[23] The RRKM calculation results are presented in Fig. 8 and in Table IV.

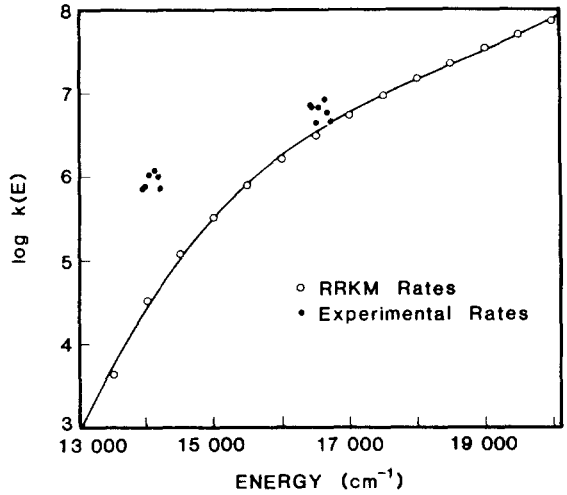

FIG. 8. Statistical RRKM rate of allyl isocyanide isomerization as a function of vibrational energy. For comparison, each experimentally measured photoisomerization rate is plotted at its photon energy.

For comparison, experimentally measured photoisomerization rates are plotted at the excitation photon energy. The experimental rates are considerably faster than the RRKM rates, although the breakdown of the single collision assumption can account for at least some of this discrepancy (see Sec. IV A). However, more significantly, the oscillations in the experimental rates are not seen in the calculated RRKM rates. Although it is not discernible from Fig. 8, the direct counting of states of the reactive complex does lead to small nonmonotonic fluctuations in the RRKM rate as more vibrational states of the complex become energetically accessible. However, these fluctuations are fairly small ($\sim 15\%$) and are damped within 300 cm^{-1} of the critical energy. Thus, the fluctuations observed in the 6–0 photolysis data

TABLE IV. Calculated RRKM reaction rates for allyl isocyanide isomerization.

E (cm^{-1})	$k(E)$ (s^{-1})
13 500	4.44×10^{3}
14 000	3.42×10^{4}
14 500	1.20×10^{5}
15 000	3.35×10^{5}
15 500	7.84×10^{5}
16 000	1.63×10^{6}
16 500	3.10×10^{6}
17 000	5.51×10^{6}
17 500	9.27×10^{6}
18 000	1.49×10^{7}
18 500	2.30×10^{7}
19 000	3.44×10^{7}
19 500	5.00×10^{7}
20 000	7.10×10^{7}

cannot be reasonably attributed to this quantum state counting effect because the photon energy exceeds the barrier by more than 2500 cm^{-1}.

IV. DISCUSSION

We consider possible explanations for the observed dependence on excitation wavelength and temperature in the overtone-pumped photoisomerization yield. We first discuss the room temperature results, then the elevated temperature work.

A. Room temperature photolyses

1. "Weak collider" effects

In the Stern–Volmer analysis presented above, the process of collisional deactivation of the vibrationally excited molecule is treated in the "single collision deactivation" limit. That is, one collision with an unexcited partner (in our case, another allyl isocyanide molecule) is assumed to be sufficient to remove enough energy to prevent isomerization. Under these conditions, we have $k_2 = Z$, where Z is the collision frequency. However, this treatment has been shown to be overly simplistic in the cases of methyl isocyanide isomerization,[25,47] the cyclobutene ring opening reaction,[48] and tert-butyl hydroperoxide decomposition.[49] Using master equation modeling of the reaction system, Miller and Chandler[47,49] have shown that the experimentally observed slopes in Stern–Volmer plots are sensitive functions of the average amount of energy transferred per collision $\langle \Delta E \rangle$, even when the excitation energy is close to the reaction threshold. Miller and Chandler also point out that linear Stern–Volmer plots are not necessarily indicative of single collision or even strong collision behavior.[47] Moreover, with excitation in the 6–0 C–H region roughly 2500 cm^{-1} above the reaction barrier, the assumption of single collision deactivation is strongly suspect. Typical values of the average energy transferred per collision inferred from master equation studies of overtone excitation are roughly 1000 cm^{-1}.

Nevertheless, the experimentally observed change in slope in the Stern–Volmer plots with excitation wavelength cannot reasonably be explained by deviations from strong collision conditions. As long as the collisional deactivation rate constant k_2 does not vary significantly over the limited energy range of an overtone region ($\sim$250 cm^{-1} out of total excitation energies of $\sim$14 000 and $\sim$16 600 cm^{-1} for 5–0 and 6–0 C–H, respectively), the observed change in slope in the Stern–Volmer plots with photon energy must be attributable to variations in $k_3(h\nu)$. Thus, the assumption of a constant deactivation rate within an overtone level should be a good approximation given the small range in excitation energies considered. Some changes in the average amount of energy transferred per collision $\langle \Delta E \rangle$ with excitation energy have been reported in the collisional quenching of azulene.[50] However, almost doubling the vibrational energy in an azulene molecule, from 17 500 to 30 600 cm^{-1}, only increased the average energy transferred in a collision with a cold azulene molecule by 17%, although other collision partners showed a somewhat greater change. Hippler, Tröe, and Wendelken[51] also have reported essentially energy independent $\langle \Delta E \rangle$ values in cycloheptatriene. Therefore, the assumption that the collisional deactivation rate constant k_2 does not change appreciably within an overtone region is likely to be valid.

2. Thermal effects and inhomogeneous broadening

Thus far, we have considered only energy provided by the photon in comparing the experimental data with the RRKM calculation. However, the molecule contains thermal vibrational energy prior to overtone excitation. This thermal energy may contribute to the reaction rate. Experimentally, Fig. 6 shows that the photoisomerization rate is indeed temperature dependent. At 293 K, allyl isocyanide has an average vibrational energy of 565 cm^{-1}. Just as in the case of removing the single collision assumption discussed above, addition of this average energy to the excitation energy will reduce the overall disparity between the calculated statistical and experimental values without explaining the experimentally observed nonmonotonic behavior. However, the contribution from thermal motion need not be the same at every excitation wavelength. Stated another way, the total vibrational energy after absorption of a photon might not vary monotonically with excitation energy. In this case, $k_3(h\nu)$ would be expected to be nonmonotonic with wavelength, as observed. This unequal distribution of thermal vibrational energy with wavelength would be a consequence of inhomogeneous contributions to the overtone width from sequence or hot bands, as discussed by von Puttkamer, Dübal, and Quack.[52]

The nature of the dominant broadening mechanism in overtone spectra of large polyatomic molecules ($\sim$100 cm^{-1} FWHM in the case of allyl isocyanide) has been the subject of considerable study,[13,36,52–60] yet remains an area of controversy. Much work has been done based on the assumption that the overtone width is entirely homogeneously broadened and that oscillator strength from the CH overtone is distributed over a dense manifold of vibrational eigenstates.[13,53] In principle, it is possible to determine experimentally the nature of the dominant broadening mechanism in overtone features by recording spectra at very low temperatures and comparing the results with room temperature spectra. Unfortunately, difficulties involving the weakness of overtone transitions and the low vapor pressures of polyatomic molecules at reduced temperatures have made such experiments rare, and no direct evidence is presently available concerning the nature of the broadening of the overtone features of allyl isocyanide.

Molecular beam cooling has been successfully used on a few systems. Some of the studied molecules, like H_2O[54] and H_2O_2,[55] show greatly reduced overtone bandwidths from beam cooling, while tetramethyldioxetane[56] changes negligibly, suggesting inhomogeneous contributions to the observed profile are small in that case. The elegant work of Page, Shen, and Lee,[57] which employed supersonic jet cooling and MPI double-resonance detection, has demonstrated that the vibrational absorption bands of benzene from the C–H fundamental up to the 3–0 C–H stretch overtone were significantly narrower at $T_{rot} = 5$ K than at room temperature. Results for the higher overtones are not yet available.

Static cooling of methane to 77 K in a photoacoustic cell has been shown to reduce the essentially featureless ~ 100 cm^{-1} wide $6\nu_1$ absorption to a series of ~ 1 GHz, Doppler-limited rovibrational lines.[58] More recent cold cell photoacoustic spectroscopy on a variety of hydrocarbons performed in this laboratory[59] has yielded a mixed picture. The effect of lowering the temperature on overtone width depends on the molecule, the overtone level, and the type of C–H oscillator excited. The extent of the change in the overtone band shape in some of the studied molecules does not appear to depend solely on the overall vibrational density of states. This suggests that the homogeneous contribution to the spectral width may be strongly dependent on the details of a particular C–H oscillator and the nature of its coupling to the other vibrational modes of the molecule. In particular, the importance of Fermi interaction between C–H stretching and bending in the overtone spectra of many systems has been discussed previously.[52,60,61]

Indirect evidence for inhomogeneous broadening in the overtone spectrum of a large polyatomic molecule comes from a study of the overtone-pumped isomerization of 1,3,5 hexatriene by Chuang and Zare.[36] A similar nonmonotonic dependence on energy was seen in the isomerization rate of this molecule to cyclohexadiene. The authors attributed this behavior to contributions from hot bands and effects from unresolved rotations.

Since the photon energy in the 5–0 C–H stretch region is very close to the critical energy for the allyl isocyanide isomerization reaction, the photolysis data collected in this region might be expected to provide an especially keen test for the RRKM calculations. Unfortunately, as discussed in Sec. III E, the value of the critical energy is not well determined and this introduces a considerable uncertainty in the calculated RRKM rate at these energies, as $k(E)$ changes rapidly near the critical energy. The decreased cross sections inferred from the Stern–Volmer plots at photolysis energies of 14 040 cm^{-1} and below (see Table III) suggest that these energies are slightly less than the critical energy because $k_{app}(0) = k_1 = \sigma(\nu)\, c$ [see Eqs. (8) and (10)] only if all photoexcited molecules react in the limit of no collisions. This will not be true if the photon energy is below the critical energy, as only molecules with enough initial thermal excitation will have sufficient energy to react. Similarly, the dramatic temperature dependence in both the Stern–Volmer slope and the intercept at 14 040 cm^{-1}, seen in Fig. 6(a), also suggests close proximity to the reaction barrier. A possible contradiction to this interpretation is the observation by Reddy and Berry of photoisomerization at photon energies down to 13 400 cm^{-1}. In addition, k_{app}^{-1} intercepts extrapolated from high pressure might be expected to be too high near the critical energy because of the negative curvature observed at low pressure in master equation modeling of overtone-pumped molecules under these conditions.[47] Further consideration of the 5–0 C–H photolysis data must await more information on the critical energy. In addition, information on the rotational states populated by laser pumping at a given wavelength might also be required, as the J dependence in the unimolecular decomposition rate of formaldehyde is reported to be large near the reaction threshold.[62] However, obtaining such information would require a very detailed understanding of the high overtone spectrum of allyl isocyanide.

The photon energy at the 6–0 C–H level is sufficiently far above the critical energy that the uncertainty in the critical energy is relatively unimportant. In this case, we may investigate whether unresolved inhomogeneous structure and thermal energy can qualitatively account for the room temperature photoisomerization data. Reference to Fig. 8 shows that the slowest experimentally measured photoisomerization rate $4.8\times10^6\ s^{-1}$ at 16 714 cm^{-1}, is only slightly faster than the rate predicted from RRKM theory at that energy, $4.0\times10^6\ s^{-1}$. The discrepancy may be attributed to an overestimate of the collisional deactivation rate, which would lead to a proportionate overestimation of $k_3(h\nu)$, or to inaccurate E_a^∞ or transition state frequencies, or to the effects of thermal vibrational energy, which effectively raises the energy at which the reaction takes place. Let us restrict our attention to this last explanation. From the RRKM $k(E)$ vs E curve, we can determine how much vibrational energy is required to achieve the experimental rate of $4.8\times10^6\ s^{-1}$, according to our statistical model for the isomerization. The statistically calculated energy for this rate is 16 770 cm^{-1}, which exceeds the photon energy by only ~ 55 cm^{-1}. Presumably, this additional energy comes from the available thermal energy. Similar calculations can be done for the other six photolysis energies and the results are given in Table V. The energies quoted in the fourth column are the differences between the energy predicted by the statistical calculation and the photon energy. The differences range from 55 to 680 cm^{-1}. These values should be compared to the average vibrational energy form allyl isocyanide, which is 575 cm^{-1} at 293 K.

It is important to note that the ΔE values quoted in Table V are only weakly dependent on such quantities as the collisional deactivation rate or the statistical modeling of the reaction. Calculations done with different physically plausible parameters give similar results. Perhaps a more serious limitation in our picture is the assumption that the excited molecules are monoenergetic. Most previous studies have assumed that the ensemble of excited molecules is the initial thermal distribution displaced by the energy of the photon,[47–49] but in this case, if the reaction rate depends only on total energy, the reaction rate would increase monotonically

TABLE V. Overtone photolysis energies in the 6–0 C–H region and estimated total vibrational energy from RRKM theory.

Excitation energy (cm^{-1})	$k_3(h\nu)$ ($10^6\ s^{-1}$)	Total vibrational energy (cm^{-1})[a]	ΔE (cm^{-1})
16 410	7.3	17 090	680
16 461	6.8	17 040	580
16 512	4.6	16 740	230
16 540	6.8	17 040	500
16 622	8.5	17 220	600
16 668	6.0	16 940	270
16 714	4.8	16 770	55

[a] Energy inferred from $k_3(h\nu)$ and RRKM calculation (see Sec. IV A).

with increasing photon energy. One might imagine that the laser could excite some fraction of molecules from each of the thermally populated vibrational energy states, yielding a distribution of reactive molecules with different energies which react at different rates. However, since we have no information about this reactive distribution or how it might vary with excitation energy, we are limited to describing the reactive population as monoenergetic. Nevertheless, despite the relatively simplistic approach employed here, we are able to get a useful qualitative measure of the possible consequences of unresolved inhomogeneous structure. Of course, this qualitative agreement by no means proves that thermal energy and unresolved inhomogeneous structure is solely responsible for the isomerization rate variations seen at room temperature. However, the results in Table V indicate that this explanation is plausible.

3. Nonstatistical effects

The final possible explanation considered here for the observed trends in the room temperature photoisomerization data is that there is unresolved homogeneous structure in the overtone spectrum of allyl isocyanide and that the rate of isomerization from a photoexcited state or set of states is not merely a function of the total energy in the molecule but also of the state or states excited. Presumably, exciting states more strongly coupled to the reaction coordinate would enhance isomerization relative to exciting states weakly coupled to the reaction coordinate. Such effects have been studied theoretically for some triatomic systems.[19,20,63,64]

The argument outlined above is essentially the explanation offered by Reddy and Berry for the overtone-induced isomerization of allyl isocyanide,[17] although they did not propose a detailed model of how the different excited C–H oscillators couple to the reaction coordinate. In a molecule as large as allyl isocyanide, this would be a considerable task, even for the simplest trajectory calculations. The results of the present work show that the variations in the isomerization rate within an overtone band are as significant as the variations between overtone peaks observed by Reddy and Berry. Therefore, the coupling of the states excited by the laser to the reaction coordinate must vary as the laser is tuned within an overtone band, according to this picture. Since we have no information at present about the nature of possible unresolved states in the overtone spectrum of allyl isocyanide and how they might couple to the reaction coordinate, we have no basis for constructing a detailed model whereby the observed trends in the photoisomerization data could be rationalized.

B. Photolyses at elevated temperatures

We undertook a limited study of the effect of temperature on the photolysis yield while exciting in the 6–0 C–H stretch region to look for possible inhomogeneous effects on the photoisomerization process. The interpretation of our results must account for changes in the collisional deactivation rate constant k_2 with increased temperature. To a first approximation, we expect the collision number and thus the collisional deactivation rate to increase with temperature as $T^{1/2}$. Thus, the increased yields seen at 353 K were measured against a "collisional clock" roughly 10% faster than at room temperature under the same conditions. Therefore, the increase in the photoisomerization rate with increasing temperature is 10% greater than is immediately apparent from the difference in slope of the Stern–Volmer lines at 293 and 353 K in Fig. 8(c).

Using the simple hot band model described above, we can estimate how much we would expect our yield to increase as a result of increased population in the initial thermal distribution of the particular hot band mode. For example, Table V indicates that the hot band at 16 668 cm^{-1} is 270 cm^{-1}. At 333 K, the thermal population of this state will increase by a factor of 1.17 relative to room temperature, while the experimental ratio $k_3(h\nu; T = 333\ K)/k_3(h\nu; T = 293\ K)$ at 16 668 cm^{-1} is 1.24 ± 0.12. Similarly, the population of a mode at 600 cm^{-1} with increase by a factor of 1.65 from 293 to 353 K. This should be compared with the experimental value of $k_3(h\nu; T = 353\ K)/k_3(h\nu; T = 298\ K)$ at 16 622 cm^{-1}, which is 1.61 ± 0.16. However, if our simple model is correct and the result of heating the sample is merely to increase the population of the state pumped by the laser, we would expect an increase in the excitation rate constant k_1, which would decrease the Stern–Volmer intercept. The isomerization rate constant $k_3(h\nu)$ would not change, according to this model, yet there is no evidence of a lowering in the k_{app}^{-1} intercept with increasing temperature in Figs. 6(b) and 6(c). This discrepancy may be a consequence of the simplicity of the model. If the laser excites several different states with a variety of energies, the total number of molecules pumped upon heating may not change greatly even though the average energy of the pumped molecule, and thus $k_3(h\nu)$, is increasing.

The temperature dependence in the photoisomerization of allyl isocyanide is consistent with inhomogeneous structure in the overtone spectrum. Please note that a purely homogeneous mechanism would predict no temperature dependence. This does not prove that homogeneous effects are absent or unimportant, but it does indicate that unresolved inhomogeneous structure in the overtone spectrum plays a significant role in the photoisomerization of allyl isocyanide.

V. CONCLUSION

The observed 6–0 C–H photolysis data of allyl isocyanide can be explained by a model which assumes that the overtone band shapes are inhomogeneously broadened. Molecules excited at different parts of the overtone band possess differing amounts of thermal vibrational energy and thus may have significantly different amounts of energy following excitation. This explanation can account for the observation that the overtone photoisomerization rate varies nonmonotonically with photolysis energy at room temperature. In addition, this model can successfully predict the observed increase in the photoisomerization rate with temperature. We therefore conclude that inhomogeneous effects can account for the photolysis data in this energy region. The 5–0 C–H photolysis data of allyl isocyanide cannot be successfully modeled until the critical energy for the isomerization

is better established. However, the interpretation of the 6–0 C–H data is unlikely to be affected by modest changes in E_0 or in the assumed form of the transition state.

ACKNOWLEDGMENTS

The authors would like to thank Deanne Snavely, David Klenerman, Jonathan Gutow, Jennifer Mihalick, David Golden, David Chandler, Hope Michelsen, and Melissa Hines for their help. This work was supported by Standard Oil (Indiana) from 1983–1986 and thereafter by the National Science Foundation under NSF CHE 85-05926.

[1]B. R. Henry and W. Siebrand, J. Chem. Phys. **49**, 5369 (1968).
[2]For recent reviews, see F. F. Crim, Annu. Rev. Phys. Chem. **35**, 657 (1984); H. Reisler and C. Wittig, *ibid.* **37**, 307 (1986).
[3]G. Herzberg, *Spectra of Diatomic Molecules* (Van Nostrand, New York, 1950).
[4]M. L. Sage and J. Jortner, Adv. Chem. Phys. **47**, 293 (1981).
[5]L. Halonen and M. S. Child, Adv. Chem. Phys. **57**, 1 (1984).
[6]P. J. Robinson and K. A. Holbrook, *Unimolecular Reactions* (Wiley–Interscience, New York, 1972).
[7]K. V. Reddy and M. J. Berry, Chem. Phys. Lett. **52**, 111 (1977).
[8]K. V. Reddy and M. J. Berry, Faraday Discuss. **67**, 188 (1979).
[9]J. M. Jasinski, J. K. Frisoli, and C. B. Moore, Faraday Discuss. **75**, 289 (1983).
[10]J. M. Jasinski, J. K. Frisoli, and C. B. Moore, J. Phys. Chem. **79**, 1312 (1983).
[11]J. M. Jasinski, J. K. Frisoli, and C. B. Moore, J. Chem. Phys. **87**, 2209 (1983).
[12]J. M. Jasinski, J. K. Frisoli, and C. B. Moore, J. Chem. Phys. **87**, 3826 (1983).
[13]K. V. Reddy, D. F. Heller, and M. J. Berry, J. Chem. Phys. **76**, 2814 (1982).
[14]D. W. Chandler, W. E. Farneth, and R. N. Zare, J. Chem. Phys. **77**, 4447 (1982).
[15]M.-C. Chuang, J. E. Baggott, D. W. Chandler, W. E. Farneth, and R. N. Zare, Faraday Discuss. **75**, 301 (1983) .
[16]H. Gutow, D. Klenerman, and R. N. Zare, J. Phys. Chem. **92**, 172 (1988).
[17]K. V. Reddy and M. J. Berry, Chem. Phys. Lett. **66**, 223 (1979).
[18]J. A. Green II and P. T. Hoffmann, *Isonitrile Chemistry*, edited by I. Ugi (Academic, New York, 1971).
[19]T. A. Holme and J. S. Hutchinson, J. Chem. Phys. **83**, 2860 (1985).
[20]T. Uzer and J. T. Hynes, in *Stochasticity and Intramolecular Redistribution of Energy*, edited by R. Lefebvre and S. Mukamel, NATO ASI Series (Reidel, Dordrecht, 1986).
[21]K. M. Maloney and B. S. Rabinovitch, *Isonitrile Chemistry*, edited by I. Ugi (Academic, New York, 1971).
[22]F. W. Schneider and B. S. Rabinovitch, J. Am. Chem. Soc. **84**, 4215 (1962).
[23]K. M. Maloney and B. S. Rabinovitch, J. Phys. Chem. **73**, 1652 (1969).
[24]J. L. Collister and H. O. Prichard, Can. J. Chem. **54**, 2380 (1976).
[25]D. L. Snavely, R. N. Zare, J. A. Miller, and D. W. Chandler, J. Phys. Chem. **90**, 3554 (1986).
[26]H. Liskow, C. F. Bender, and H. F. Schaefer III, J. Chem. Phys. **57**, 4509 (1972).
[27]P. Saxe, Y. Yamaguchi, P. Pulay, and H. F. Schaefer III, J. Am. Chem. Soc. **102**, 3718 (1980).
[28]A. Zewail, Faraday Discuss. **75**, 342 (1983).
[29]G. D. Hartman and L. M. Weinstock, Org. Syn. **59**, 183 (1980).
[30]W. Lieke, Justus Liebig Ann. Chem. **112**, 316 (1859).
[31]E. Lücher, P. Korpuin, H.-J. Coufal, and R. Tilgner, *Photoacoustic Effect: Principles and Applications* (Vieweg, Baunschweig, 1984).
[32]A. Rosencwaig, *Photoacoustics and Photoacoustic Spectroscopy* (Wiley, New York, 1980).
[33]Y.-H. Pao, *Optoacoustic Spectroscopy and Detection* (Academic, New York, 1977).
[34]A. M. Smith, U. G. Jørgensen,, and K. K. Lehmann, J. Chem. Phys. **87**, 5649 (1987).
[35]L. P. Giver, J. Quant. Spectrosc. Radiat. Transfer **19**, 311 (1978).
[36]M.-C. Chuang and R. N. Zare, J. Chem. Phys. **82**, 4791 (1985).
[37]Figure 2(c) is reproduced from Ref. 17. 6–0 C–H spectra obtained in this lab are in reasonable agreement but with reduced signal to noise.
[38]A. L. Verma, J. Mol. Spectrosc. **39**, 247 (1971).
[39]J. S. Wong and C. B. Moore, J. Chem. Phys. **77**, 603 (1982).
[40]J. Casanova, N. D. Werner, and R. E. Schuster, J. Org. Chem. **31**, 3473 (1966).
[41]M. J. Glionna and H. O. Pritchard, Can. J. Chem. **57**, 2482 (1979).
[42]S. F. Stein and B. S. Rabinovitch, J. Chem. Phys. **58**, 2438 (1973).
[43]J. L. Duncan, D. C. McKean, M. W. Mackenzie, and J. P. Peña, J. Mol. Spectrosc. **76**, 55 (1979).
[44]G. Herzberg, *Infrared and Raman Spectra* (Van Nostrand, New York, 1945), p. 333.
[45]S. Glasstone, K. J. Laidler, and H. Eyring, *The Theory of Rate Processes* (McGraw–Hill, New York, 1941), p.195.
[46]K. M. Maloney and B. S. Rabinovitch, J. Phys. Chem. **73**, 1652 (1969).
[47]J. A. Miller and D. W. Chandler, J. Chem. Phys. **85**, 4502 (1986).
[48]J. E. Baggott, Chem. Phys. Lett. **119**, 47 (1985).
[49]D. W. Chandler and J. A. Miller, J. Chem. Phys. **81**, 455 (1984).
[50]M. J. Ross, J. R. Pladziewicz, and J. R. Barker, J. Chem. Phys. **78**, 6695 (1983).
[51]H. Hippler, J. Tröe, and H. H. Wendelken, J. Chem. Phys. **78**, 6709 (1983).
[52]K. von Puttkamer, H.-R. Dübal, and M. J. Quack, Faraday Discuss. Chem. Soc. **75**, 157 (1983).
[53]K. L. Bintz, D. L. Thompson, and J. W. Brady, J. Chem. Phys. **86**, 4411 (1987), and references therein.
[54]C. Douketis, D. Anex, G. Ewing, and P. J. Reilly, J. Chem. Phys. **89**, 4173 (1985).
[55]L. J. Butler, T. M. Ticich, M. D. Likar, and F. F. Crim, J. Chem. Phys. **85**, 2331 (1986).
[56]E. S. McGinley and F. F. Crim, J. Chem. Phys **85**, 5741 (1986).
[57]R. H. Page, Y. R. Shen, and Y. T. Lee, Phys. Rev. Lett. **59**, 1293 (1987).
[58]G. J. Scherer, K. K. Lehmann, and W. Klemperer, J. Chem. Phys. **81**, 5319 (1984).
[59]M. Crofton, C. Stevens, D. Klenerman, J. H. Gutow, and R. N. Zare (in preparation).
[60]J. Segall, R. N. Zare, H. R. Dübal, M. Lewerenz, and M. Quack, J. Chem Phys. **86**, 634 (1987).
[61]W. H. Green, W. D. Lawrance, and C. B. Moore, J. Chem. Phys. **86**, 6000 (1987).
[62]J. Tröe, J. Phys. Chem. **88**, 4375 (1984).
[63]T. Uzer and J. T. Hynes, Chem. Phys. Lett. **113**, 483 (1985).
[64]J. S. Hutchinson, J. Chem. Phys. **85**, 7087 (1987).